CRYSTAL GROWTH & DESIGN

Article

pubs.acs.org/crystal

Regulating Nucleation Kinetics through Molecular Interactions at the Polymer–Solute Interface

Efrem Curcio,[†,‡] Vilmalí López-Mejías,[§] Gianluca Di Profio,[‡] Enrica Fontananova,[‡] Enrico Drioli,[†,‡] Bernhardt L. Trout,[§] and Allan S. Myerson*[,§]

[†]Department of Environmental and Chemical Engineering, University of Calabria, via P. Bucci CUBO 45A, 87036 Rende, Cosenza, Italy

[‡]Institute on Membrane Technology, National Research Council of Italy (ITM-CNR), via P. Bucci CUBO 17/C, 87036 Rende, Cosenza, Italy

[§]Department of Chemical Engineering, Massachusetts Institute of Technology, E19-502B, 77 Massachusetts Avenue, Cambridge, Massachusetts 02139-4307, United States

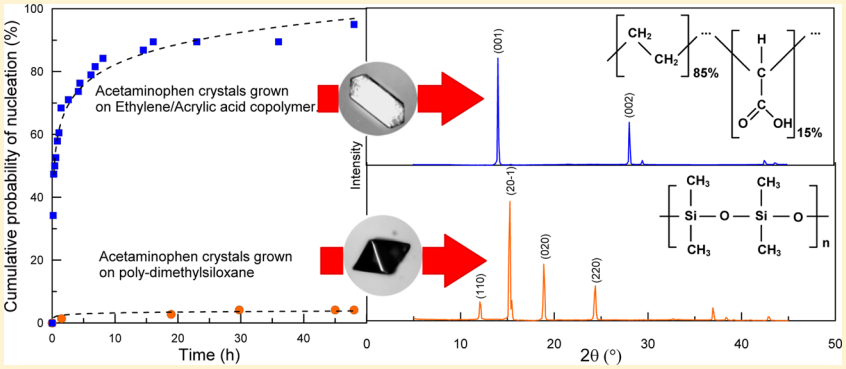

ABSTRACT: Heterogeneous nucleation is ubiquitous both in nature and in industrial practice; therefore, the ability to inhibit or enhance the kinetics of a crystallization process is essential in many scientific and technological areas. In order to better understand the role of surface functionality in regulating the nucleation rate, six commercially available polymers have been used as heteronucleants of acetaminophen (ACM) molecules: polydimethylsiloxane (PDMS) with siloxane functional groups Si–O–Si forming the backbone of silicones, partially fluorinated elastomer polyvinylidenedifluoride (PVDF), polystyrene (PS) having weak electron-donor phenyl rings, poly(*n*-buthyl methacrylate) (P*n*BMA) showing ester functionality, polyimide (PI) that includes both hydrogen-bond acceptor imide functionality and carbonyl groups, ethylene/acrylic acid (EAA) copolymer with carboxyl moiety. Experimental results from induction time statistics, van Oss–Chaudhury–Good model of surface energetics, and powder X-ray diffraction (PXRD) analysis showed that polymeric interfaces promoting specific acid–base interactions and directionally ordered reorganization of molecules led to enhanced nucleation kinetics, while the formation of nuclei was retarded on hydrophobic films that did not induce preferential orientations of the crystalline facets.

INTRODUCTION

Heterogeneous nucleation is ubiquitous and difficult to control. In industrial practice, primary nucleation essentially takes place via heterogeneous mechanism on foreign surfaces such as impurities, impellers, vessel walls, etc.[1] Uncontrolled crystalline deposits of sparingly soluble salts (mostly $CaCO_3$, $CaSO_4$), usually referred to as scaling, are responsible for losses of water permeability in membrane desalination operations[2] and for heat transfer inefficiency in thermal processes.[3] In medicine, biomineralization control is relevant in designing efficient anticalcification therapies for pathological hydroxyapatite deposition diseases such as osteoarthritis due to cartilage calcification or mineral deposits in the joints.[4] Stabilization of crystalline pharmaceutical products and inhibition of unintended polymorphic transformations can be obtained by heteronucleation induced by nonsoluble polymers with tunable polarity of surface functional groups.[5]

In general, the ability to control the nucleation process occurring on foreign surfaces—both in terms of inhibition or enhancement of crystallization rate—is essential in many scientific and technological fields. Despite its pervasive incidence, however, the role of surfaces in heterogeneous nucleation is still poorly understood and not systematically investigated.

Fermani et al. (2001) showed that the crystallization of concanavalin A and lysozyme on polymeric films containing ionizable groups (such as sulfonated polystyrene, cross-linked

Received: October 18, 2013
Revised: December 19, 2013
Published: December 30, 2013

gelatin films with adsorbed poly-L-lysine or entrapped poly-L-aspartate, and silk fibroin with entrapped poly-L-lysine or poly-L-aspartate) resulted in lower induction times and higher nucleation densities with respect to reference siliconized coverslip.[6]

Apatite nucleation is enhanced by surfaces containing silanol (Si−OH) groups or silicate ions adsorbed on them.[7]

Diao et al. (2011) used nonporous cross-linked poly-4-acryloylmorpholine (PAM), poly-2-carboxyethyl acrylate (PCEA), poly-4-hydroxylbutyl acrylate (PHBA), and polystyrene (PS) substrates to control the nucleation rate of aspirin; induction time measurements showed that polymer films which are polar and contain multiple hydrogen-bonding sites exhibit higher nucleation activity compared to less polar films.[8]

Polymer-induced heteronucleation (PIHn) was proven as an effective method for controlling the nucleation rate across a broad range of materials.[9] Amorphous surfaces can promote heterogeneous nucleation merely by lowering the surface energy of aggregating molecules (nonspecific adsorption) or by structural matching driven by specific polymer−molecule interfacial interactions according to a mechanism analogous to epitaxial growth. PIHn capability of polymorph selection, kinetically driven by the preferential aggregation of molecules along specific crystalline facets, corroborates these assumptions.[10] Hydrophobic polymeric membranes made in polyvinylidenedifluoride (PVDF), polydimethylsiloxane (PDMS), and Hyflon proved their ability to control the kinetics of lysozyme crystallization from solution by tuning surface energy and morphology.[11,12] Recent studies explored the combined effect of topography and hydrophobic−hydrophilic character of polymeric membranes on the nucleation rate of small organic molecules such as acetaminophen, acetylsalicylic acid, and glycine.[13]

In addition, theoretical investigations recently contributed to a better understanding of heterogeneous nucleation phenomena at the molecular level. Studies based on molecular dynamics suggested a possible correlation between binding affinity of aspirin molecules to the local area of the best sites of PAM, PCEA, PHBA, and PS surfaces (ranging from −20.4 ± 1.0 to −13.6 ± 1.1 kcal/mol) and nucleation rate.[14] Moreover, a weak trend of the distance order parameters was found to be analogous to that of the heterogeneous nucleation rate.[15]

Further and deeper investigations focusing on the effect of surface chemistry, stimulated by the lack of fundamental knowledge and absence of an accurate description of early stage formation of clusters, might contribute to the elucidation of thermodynamic and kinetic mechanisms of heterogeneous nucleation.

With the aim to investigate the complex mechanisms of solid phase formation due to specific solute−surface interactions, six commercially available polymers of technological interest have been used in this work to prepare flat films for crystallization tests. The polymers investigated here are polydimethylsiloxane (PDMS) with siloxane functional groups Si−O−Si forming the backbone of silicones, partially fluorinated elastomer polyvinylidenedifluoride (PVDF), polystyrene (PS) having weak electron-donor phenyl rings, poly(*n*-buthyl methacrylate) (P*n*BMA) showing ester functionality, polyimide (PI) that includes both hydrogen-bond acceptor imide functionality and carbonyl groups, ethylene/acrylic acid (EAA) copolymer with only the carboxyl moiety. Molecular structures of the above-mentioned polymers are shown in Figure 1. Acetaminophen (ACM), a common antipyretic and analgesic drug, was chosen as the model compound for this investigation. Heterogeneous nucleation kinetics was experimentally investigated in terms of induction time statistics, contact angle analysis treated by the van Oss−Chaudhury−Good model,[16] and determination of the preferred crystal orientation by PXRD analysis with the aim to clarify the role of the surface chemistry in the polymer-induced heteronucleation of ACM molecules from solution on solid substrates.

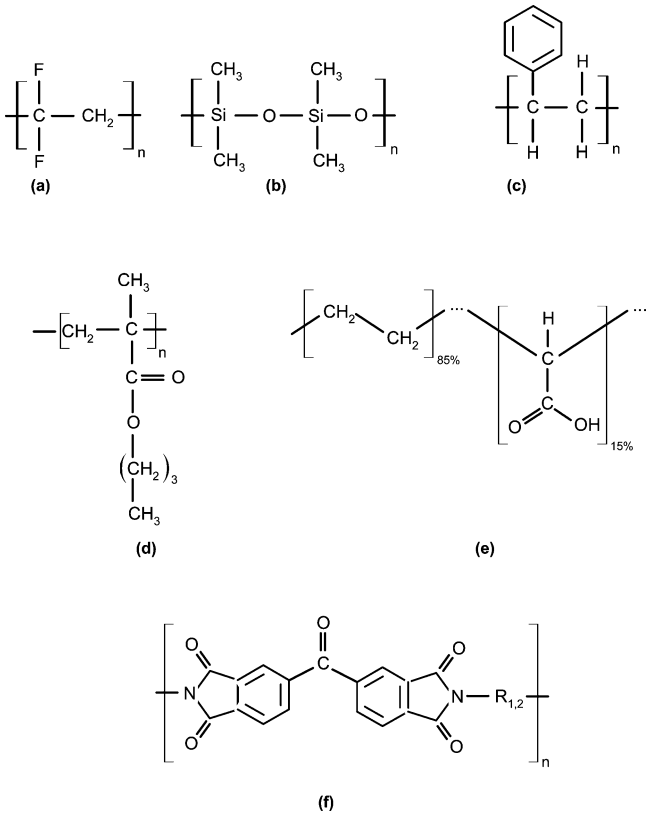

Figure 1. Molecular structures of polymers used in this work: (a) polyvinylidene difluoride (PVDF); (b) polydimethylsiloxane (PDMS); (c) polystyrene (PS); (d) poly *n*-butyl methacrylate (P*n*BMA); (e) ethylene/acrylic acid (EAA) copolymer; (f) polyimide (PI).

MATERIALS AND METHODS

Crystallization Solution. Acetaminophen (ACM), purchased from ICN Biomedicals Inc. (USA), was dissolved at 60 °C for 1 h in deionized water (18.3 MΩ) obtained by Millipore Milli-Q purification system. Before crystallization tests, the solution (30 g ACM/kg H_2O, supersaturation ratio: 3.18[17]) was filtered through Acrodisc 0.2 μm PTFE syringe filter (Pall Life Science, USA).

Induction Time Statistics. Polymeric solutions of poly(*n*-buthyl methacrylate) (P*n*BMA) and polystyrene (PS), both purchased from Scientific Polymer Products Inc. (USA), were prepared by dissolution in toluene (Sigma-Aldrich Chemical Co., USA) with polymer weight fraction of 10% (w/w) at 60 °C. Poly vinylidene fluoride (PVDF) and ethylene/acrylic acid (15%) copolymer (EAA), both purchased from Scientific Polymer Products Inc. (USA), were dissolved at 60 °C in dimethylformamide and *n*-xylene (Sigma-Aldrich Chemical Co., USA), respectively, with a polymer weight fraction of 10% (w/w).

Five hundred microliters of a polymeric solution was dispensed in a 1.0 mL borosilicate glass vial at room temperature. A two-day wait in a fume hood was typically necessary to complete solvent evaporation and to form a homogeneous polymeric film at the wall of the vial. To remove the residual solvent, all vials were annealed at 70 °C in a vacuum drying oven (ADP-31, Yamato Scientific America Inc., USA) for 3 h. Polydimethylsiloxane (PDMS) solution was prepared by

dx.doi.org/10.1021/cg4015543 | *Cryst. Growth Des.* 2014, 14, 678−686

mixing Silgard silicone elastomer base and curing agent at room temperature and with a volumetric ratio of 10:1. The solution was shaken vigorously with a wooden stick for about 30 s, allowed to stand for 10 min under a fume hood, dispensed in vials in amount of 200 μL, and annealed according to procedure before described.

P84 polyimide, kindly supplied by HP Polymer Inc. (Lewisville, Texas, USA) in powder grain sizes of 200 mesh, was dissolved in dimethylformamide (Sigma-Aldrich Chemical Co., USA) with a polymer weight fraction of 10% (w/w) at 40 °C and gently stirred for about 24 h. The solution was cast on a glass plate and then immersed in deionized water for 15 min to form a polymeric film by diffusion induced phase separation (DIPS) in antisolvent. The film obtained was used to cover walls of the crystallization vials.

In a typical induction time measurement test, 80 vials—each one charged with 800 μL of the crystallization ACM solution—were placed in a perforated metal plate kept at 10 ± 0.1 °C by recirculating water from a refrigerated bath; the temperature of the ACM solution, monitored by a thermocouple probe, was stabilized in about 5 min. The optical images were collected for 48 h, with a time interval of 5 min, by a Zeiss Axiovert 200 microscope (Carl Zeiss International, USA), fully automated, and controlled via AxioVision software, operated in transmission mode. Recorded frames were scrutinized in order to count the number of vials crystallized within the time elapsed.

Contact Angle Measurement. Contact angle (θ) was measured by sessile drop method at room temperature using a KRÜSS Gmbh (Germany) Drop Shape Analysis DSA10 system. In a typical test, a 3 μL droplet size was lowered onto the polymer surface, and images were recorded until contact angle stabilization; contact angle for each probing liquid was obtained from the average of five measurements. Water, glycerol, and diiodomethane (Sigma-Aldrich-USA) were used as probing liquids to determine the apolar Lifshitz–van der Waals γ^{LW}, the acid–base γ^{AB}, the acid (electron-attractor) γ^{+}, and the base (electron-donor) γ^{-} components of the surface free energy for both polymer film and ACM solution, according to the van Oss–Chaudhury–Good model.[16] Values of surface tension components and parameters for reference liquids are in ref 18.

In particular, from diiodomethane (apolar test liquid) contact angle:

$$\gamma_s^{LW} = \frac{\gamma_l^{LW}(1 + \cos\theta)^2}{4} \tag{1}$$

Remaining components were calculated from contact angles to two polar liquids (water and glycerol):

$$\gamma_l(1 + \cos\theta) = 2\left(\sqrt{\gamma_s^{LW}\gamma_l^{LW}} + \sqrt{\gamma_s^{+}\gamma_l^{-}} + \sqrt{\gamma_s^{-}\gamma_l^{+}}\right) \tag{2.1}$$

and

$$\gamma_s^{AB} = 2\sqrt{\gamma_s^{+}\gamma_s^{-}} \tag{2.2}$$

In eqs 1 and 2, subscripts s and l indicate the solid and liquid phase, respectively.

Powder X-ray Diffraction Measurement. The preferred orientation of the crystal nucleated on the flat polymer films was investigated by powder X-ray diffraction (PXRD) analysis of polymer coated glass slides.

A few microliters of polymeric solutions (3% w/w) were pipetted onto rectangular 22 × 40 mm coverslips (VWR International, USA) and spin-coated at a rotation rate of 2500 rpm for 40 s (Laurell Technologies Corp., USA. model WS-650 MZ − 23 NPP/LITE) under N_2 atmosphere and room temperature. PDMS slides were prepared by deep coating, followed by annealing according to the protocol previously described. Coated slides were annealed at 70 °C under a vacuum for 4 h. In each test, a single slide was immersed in a 50 mL borosilicate glass vial containing the ACM solution (30 g ACM/kg H_2O) at 10 °C; the slide was placed in an almost vertical position in order to minimize the risk of deposition of crystals nucleated from the bulk of the solution.

Patterns were collected at room temperature by a PANalytical X'Pert PRO Theta/Theta PXRD system with Cu as the anode material and X'Celerator high-speed detector, under Stage Flat Sample configuration, 2θ scan range from 5° to 45°. The molecular views of the preferred orientation faces found by PXRD were observed in Material Studio v6 (Accelrys Software Inc., USA).

RESULTS AND DISCUSSION

Induction Time Statistics. Nucleation is inherently a stochastic event and a energy-activated process. In particular, the aleatory nature of the nucleation stage reflects the variability of induction time measurements, that is, the period elapsed from attainment of a given supersaturation until the formation of crystals with critical size, in crystallization tests carried out at constant supersaturation. On this basis, the investigation of crystal nucleation rates from experimentally determined probability distribution of induction times was recently proposed.[19]

The cumulative probability distribution for the nucleation induction time of ACM from solution at a constant supersaturation ratio of 3.18, experimentally determined from at least 64 individual experiments per polymeric surface, is reported in Figure 2. Crystallization conditions, that is, starting concentration, volume (800 μL) and temperature (10 °C), were carefully selected with the aim to suppress bulk nucleation and to observe the formation of ACM crystals in at least 4 out of 64 monitored vials (>5%) within 48 h. No crystals were observed in vials without polymer surface. The plot of the cumulative probability distribution was obtained from the nucleation time inspected by time-lapse optical microscopy. It is therefore assumed that, for ξ isolated experiments, the probability P that a successful crystallization event ξ^{+} occurs within the time t is given by

$$P(t) = \frac{\xi^{+}(t)}{\xi} \tag{3}$$

This approach, based on a Poisson-type probability distribution for independent events, is valid under the assumptions of a fast crystal growth and a high heat transfer rate. Diao et al. (2011) demonstrated that both conditions are verified for millimeter-sized glass vials in which crystals grow up to a detectable size within 10–15 min, that is, about 2 orders of magnitude less than the measured induction times.[8]

Figure 2 shows that ACM nucleation induction rate is drastically reduced when PDMS and P*n*BMA are used as heteronucleant polymers, with a cumulative probability value (after 45 h) of 4.1% and 11.3%, respectively. It can be inferred that PDMS and P*n*BMA polymeric surfaces, exhibiting a low plateau for the probability function, act as an inhibitor for ACM nucleation.

PS surface was used as a control due to high chemical inertness and absence of polar groups in the polymer chain (phenyl ring has just a very weak electron-donor behavior), thus resulting in low acid–base components of the surface tension (Table 2) and, ultimately, in feeble polymer–solute interactions. PS-coated vials show a cumulative probability value of 35% at 42 h. PVDF and PI surfaces, exhibiting a similar ability to induce the formation of nuclei, show increased values of probability: 54% (after 42 h) and 62% (after 45 h), respectively. The EAA copolymer was the most effective polymer in promoting ACM nucleation, and 95% of the 64 vials analyzed produced crystals within 2 days.

Measurements of average induction time via probability distribution of crystallization events allow a quantitative evaluation of the effect of polymer-solute interactions on the kinetics of heterogeneous nucleation. If assuming that, at

dx.doi.org/10.1021/cg4015543 | Cryst. Growth Des. 2014, 14, 678–686

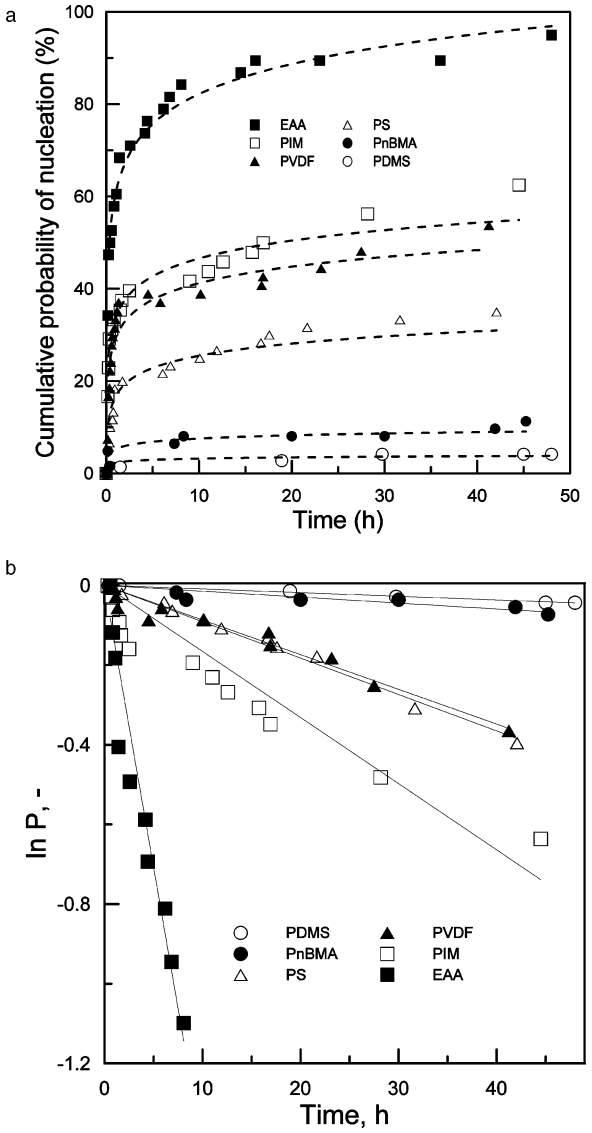

Figure 2. (a) Percentage of samples/vials crystallized (tests on 64 vials) on different polymeric surfaces as a function of time. Experimental conditions: 30 g ACM/kg H_2O, 10 °C, 800 μL solution. (b) Linear regression of probability data P according to the formula ln $P = -t/\tau$. Crystallization conditions: 30 g ACM/kg H_2O, 10 °C, 800 μL solution. Samples crystallized within 10 min have been removed from the data set.

constant supersaturation, the formation of a nucleus is an independent and random event, and if ν is the average number of nucleation events in a given interval of time, then the probability P_n of forming n nuclei within the time t is described by the Poisson distribution:[19]

$$P_n = \frac{\nu^n}{n!}e^{-\nu} \tag{4.1}$$

Finally, the probability of observing no nucleation event (P) within time t is obtained by setting $n = 0$ and $\nu = t/\tau$:

$$P = e^{-t/\tau} \tag{4.2}$$

According to Figure 2b, the average induction time (τ) is calculated by the linear regression of probability data plotting ln P as a function of t; a high value of straight-line slope corresponds to a low induction time. An acceptable agreement between model and experimental data ($R^2 > 0.9$) confirms the validity of assumptions made in order to effectively apply Poisson distribution. Induction times for ACM nucleation in polymer-coated vials at constant supersaturation, calculated by linear fit of the logarithmic form of eq 4.2 to the experimentally obtained distributions, are reported in Table 1. Contact angles, used for a preliminarily correlation analysis of nucleation rate on surfaces, are also listed in Table 1.

Table 1. Estimated Average Induction Time (τ, from eq 4.2) and Contact Angle (θ, °) of ACM Solutions (30 g ACM/kg H_2O) on Six Commercially Available Polymeric Surfaces

polymeric surface	average induction time (τ, h)	contact angle (θ, °)
polydimethylsiloxane	1310	95.9 ± 1.6
poly *n*-butyl methacrylate	478	81.4 ± 1.2
polystyrene	117	80.3 ± 2.3
polyvinylidene difluoride	101	73.9 ± 1.1
polyimide	67.6	56.6 ± 2.4
ethylene/acrylic acid (15%) cop.	11.5	99.8 ± 4.0

As from Table 1, copolymer EAA exhibits a strong hydrophobic behavior characterized by the highest measured ACM contact angle (99.8° ± 4.0). Although this value differs by only 4% from ACM contact angle on PDMS surface, the average induction time of ACM crystals nucleated on EAA surface (11.5 h) is 2 orders of magnitude lower than on PDMS film. Coherently, Trasi et al. (2012) observed that poly acrylic acid (PAA) increases nucleation rate of acetaminophen, and FTIR analysis showed that H-bonds that PAA forms with amorphous paracetamol are stronger than the hydrogen bonding occurring between drug molecules themselves.[20]

ACM nucleation rates on PS and P*n*BMA films also show a remarkable diversity in terms of average induction time (~2 and 8 h, respectively) despite the negligible difference in contact angles.

In general, these data substantiate the high sensitivity of heterogeneous nucleation to specific chemical interactions between crystallizing molecules and solid substrates.

Surface Energy Components. With the aim to identify a possible correlation between physicochemical properties of the polymeric surfaces and the nucleation rate of ACM, the contact angles of three different liquids (water, glycerol, and diiodomethane) were measured to obtain the apolar Lifshitz−van der Waals and the Lewis acid−base components of the surface free energy of the polymer.

Although surface tension analysis cannot provide a reliable calculation of induction time, the characterization of surface free energy components is recognized as a key to interpret intermolecular phenomena occurring at solid interfaces. This approach has been used in several applications: understanding the role of interfaces in heterogeneous nucleation,[21] inspecting formulation parameters of the spray-dried microparticles and their potential for adhesion to specific substrates,[22] evaluating membrane cytocompatibility by assessing adhesion and liver specific functions of isolated rat hepatocytes,[23] etc. In this work, the van Oss−Chaudhury−Good model is adopted in order to discriminate the relatively nonspecific dispersion attractive forces as well as the specific acid (electron-acceptor)−base (electron-donor) interactions across interfaces.

dx.doi.org/10.1021/cg4015543 | *Cryst. Growth Des.* 2014, 14, 678−686

Table 2. Surface Tensions Calculated According to van Oss−Chaudhury−Good Model[16] [a]

olymer	θ_w (°)	θ_{gly} (°)	θ_{dim} (°)	γ_s^{LW} (mJ/m^2)	γ_s^+ (mJ/m^2)	γ_s^- (mJ/m^2)	γ_s^{AB} (mJ/m^2)
polydimethylsiloxane	108 ± 0.3	103 ± 2.7	70.1 ± 1.1	22.8	1.52	0.481	1.71
poly *n*-butyl methacrylate	80.3 ± 2.3	63.9 ± 1.4	40.6 ± 3.9	39.3	3.44	0.593	2.86
polystyrene	78.9 ± 1.7	53.8 ± 1.7	30.1 ± 0.99	44.2	1.29	1.70	2.97
polyvinylidene difluoride	83.9 ± 1.5	82.9 ± 2.9	66.0 ± 1.4	25.1	10.9	0.01	0.135
polyimide	75.7 ± 0.9	45.1 ± 3.8	37.3 ± 1.8	40.9	1.15	3.99	4.28
ethylene/acrylic acid (15%) cop.	119 ± 1.8	117 ± 1.7	51.6 ± 4.7	33.4	0.49	5.33	3.27

[a] θ: contact angle, γ: surface tension. Subscripts w: water, gly: glycerol, dim: diiodomethane, s: polymer surface. Superscripts LW: apolar Lifshitz−van der Waals component, AB: acid−base component, +: acid (electron-acceptor) component, −: base (electron-donor) component.

The ACM solution used in crystallization tests (30 g ACM/kg H_2O) exhibits a slightly acid behavior ($pK_a \approx 9.7$, pH = 5.1). It is therefore expected that surfaces with prevalent base (electron-donor) component γ_s^- will exhibit stronger interactions with ACM molecules, thus resulting in higher nuclei density.

As reported in Table 2, the calculated value of γ_s^- for PDMS surface, characterized by the highest induction time (1310 h), ranks fifth among the six polymers investigated. The value of Lewis acid component (1.52 mJ/m^2) is higher than the corresponding base component due to the weakly acidic contribution of silanol groups. This parameter, in conjunction with the high contact angle of ACM on PDMS (95.9° ± 1.6), is coherent with a reduced interaction between polymer surface and ACM molecules. The value of apolar Lifshitz−van der Waals component for PDMS, as reported in Table 2, is in agreement with those measured by Martinelli et al.:[24] 18.0 and 21.8 mJ/m^2 for dry and wet conditions, respectively.

P*n*BMA shows a higher acid component (3.44 mJ/m^2) and a lower basic component (0.593 mJ/m^2) than polystyrene (1.29 and 1.70 mJ/m^2, respectively), despite having very similar values of ACM contact angle. The different acid−base interactions between polymeric surfaces and ACM might explain the higher induction time (+400%) and the lower nuclei density (−58%) of P*n*BMA with respect to PS. The prevalent Lewis acid contribution in P*n*BMA is due to the moderately electron-withdrawing behavior of ester groups. Calculated nonpolar contribution for P*n*BMA are coherent with literature values spanning from 34 to 36.5 mJ/m^2 as reported by Wu[25] and Pritykin.[26] Data on PS are in agreement with those from Morra et al.[27] who reported a γ_s^{LW} of 38.4 mJ/m^2. The higher base component with respect to the acid one might be attributed to the very weak electron-donor action of the benzene ring.

The PVDF surface has the lowest acid−base component γ_s^{AB} among the investigated polymers as a result of the electron-donor component that approaches zero. Values measured are consistent with those reported by Morra et al.:[27] γ_s^{LW} = 28.6 mJ/m^2, γ_s^+ = 10.5 mJ/m^2, γ_s^- = 0.08 mJ/m^2. The highest value of the electron-acceptor component is related to the fact that fluorine is the most electronegative element, thus resulting in preferential hydrogen-bond interactions with the hydroxyl group in the ACM molecule (as confirmed by X-ray diffraction data discussed below) that increase the density of nuclei (10.7 ± 0.61 cm^{-2}) with respect to the previously discussed polymeric surfaces.

PI surface exhibits a significant sensitivity to acid−base interactions (high γ_s^{AB}). The prevalence of the Lewis-base component with respect to the corresponding acid component (+345%) promotes significant interactions between solid interface and the weakly acidic ACM molecules; this is consistent with the experimental observations of high nuclei density (15.2 ± 1.2 cm^{-2}) and short induction time (67.6 h). The strong Lewis-base component (γ_s^- = 3.99 mJ/m^2), mostly due to the electron-donor behavior of nitrogen in the imide functional group, is not far from the value of 6.0 mJ/m^2 reported by Gotoh.[28]

EAA copolymer surface has the highest Lewis-base component γ_s^+; this might explain the strong interaction with ACM molecules so resulting in the highest nuclei density (20.9 ± 2.4 cm^{-2}) and the shortest induction time (11.5 h) observed, despite the high contact angle value (99.8° ± 4.0). The calculated electron-donor component is in good agreement with the value of 6 mJ/m^2 reported by Lloyd and Coleman (2000) for a 15% of acrylic acid in the EAA copolymer.[29]

Preferential Orientations. With the aim to further investigate the influence of specific intermolecular interactions between ACM and a polymer surface during nucleation, PXRD was used to identify preferred orientation (PO) of crystal facets on solid substrates. This is an indication of preferential interactions between the forming nuclei and the surface at the interface leading to aggregation and therefore crystal formation. Recently, this approach has been used to study the preferential nucleation of aspirin on polymer films obtained by cross-linking of 4-acryloylmorpholine, 2-carboxyethyl acrylate, and 4-hydroxybutyl acrylate,[8] the phase-selective crystallization of ACM using poly(*n*-butyl methacrylate) and poly(methyl-methacrylate) as heteronuclei,[9] and the soft-confined nucleation of aspirin and acetaminophen in cross-linked homopolymer gels of poly(ethylene glycol) diacrylate (PEGDA) and copolymers of PEGDA and 4-acryloylmorpholine.[30]

PXRD analysis confirms that preferred orientation occurs when most of the polymeric surfaces are used as heteronucleants during ACM crystallization. The level of PO is dependent on the strength of the intermolecular interactions occurring at the polymer−crystal interface during nucleation. The strength varies from nonspecific adsorption (PDMS, P*n*BMA, and PS) to the oriented arrangement of molecules in the crystalline lattice (EAA, PI, and PVDF). With only one exception, all of the surfaces used in this investigation produced the thermodynamically stable monoclinic, ACM form I. XPRD diffraction patterns for the six investigated polymer surfaces are reported in Figure 3a−c.

PXRD analysis of crystals nucleating on hydrophobic EAA surface reveals two predominant reflections at 14.1° (001) and 28.1° (002), indicating a strong orientation of ACM crystals along {001}. Referring to Figure 4a, the hydroxyl groups of the ACM molecules aligned along this plane appear perpendicularly oriented toward the polymeric surface, thus indicating that EAA copolymer is interacting through hydrogen-bonding. An optical micrograph of ACM crystals grown on EAA film is reported in Figure 5.

dx.doi.org/10.1021/cg4015543 | Cryst. Growth Des. 2014, 14, 678−686

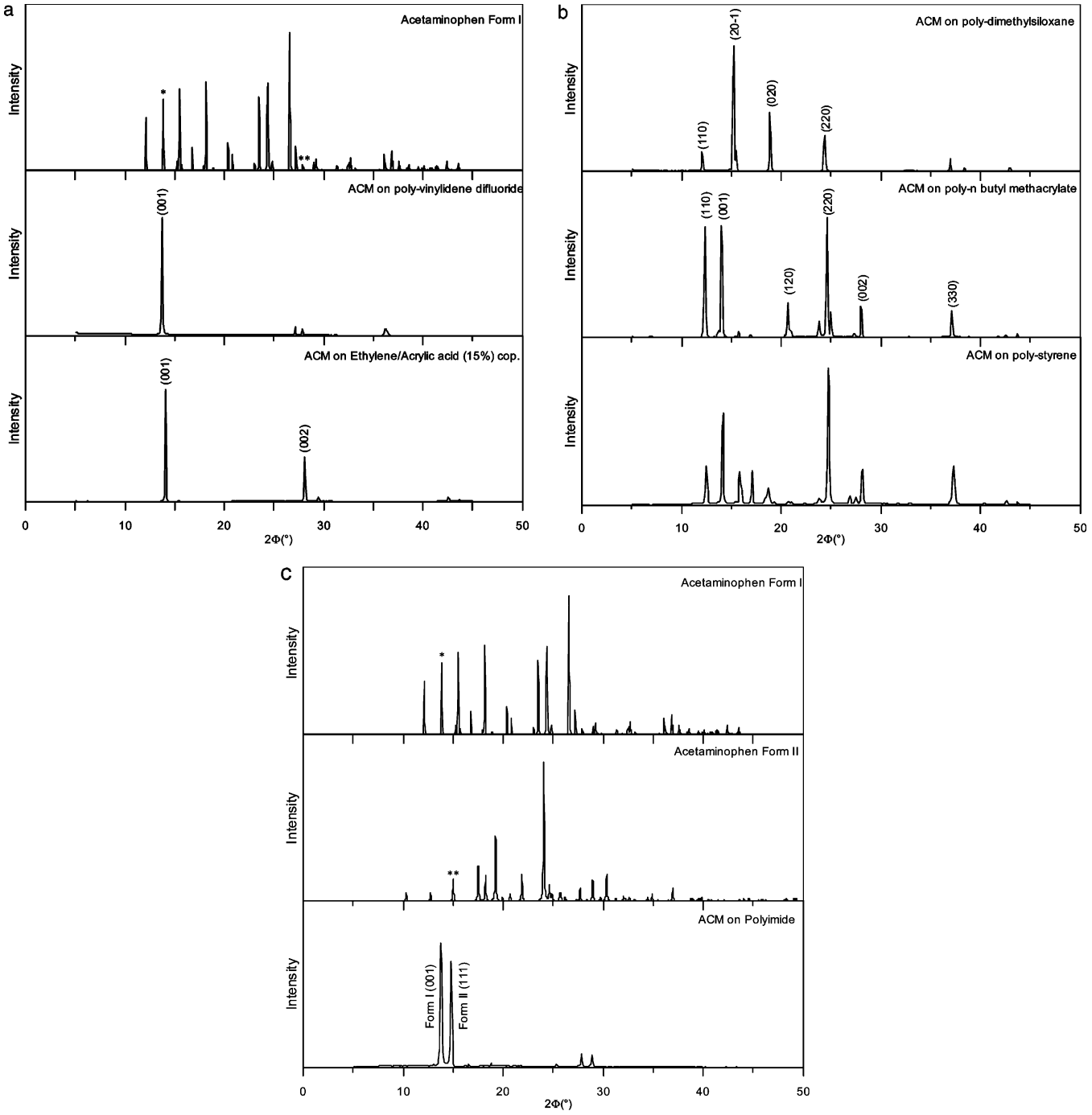

Figure 3. (a) Preferential orientation of acetaminophen (ACM) crystals nucleated on PVDF (center) and EAA copolymer (bottom) surfaces. Experimental PXRD patterns are compared to the calculated PXRD pattern ACM Form I (top) obtained from the crystallographic information file. (b) PXRD diffractograms of ACM crystals nucleated on PDMS (top), P*n*BMA (center), and PS (bottom) surfaces showing a low degree of preferred orientation along a specific crystallographic plane. (c) PXRD diffractograms show concomitant polymorphism in acetaminophen (ACM) crystals grown on polyimide (PI) surface. The experimental PXRD pattern is compared to the calculated PXRD pattern ACM Form I (top) and Form II (center) obtained from the crystallographic information files.

On the other hand, the PXRD pattern of ACM crystals nucleated on hydrophobic PDMS surface (contact angle: 95.9 ± 1.6°) exhibits four major reflections occurring at 12.1° (110), 15.4° (20−1), 18.9° (020), and 24.4° (220). As a consequence, there is no evidence for a prevalent crystal orientation along a specific crystallographic plane (Figure 5). Referring to Figure 4b, reflections whose linear combinations correspond to vector direction {110} do not represent specific interactions: some ACM molecules are parallel the polymer surface, others have hydroxyl and methyl groups alternatively redirected toward the solid substrate. The main peak at 15.4°, related to orientation along $\{20\bar{1}\}$, reveals that methyl groups and amide portion in ACM molecule are perpendicularly aligned to the PDMS surface (Figure 4c). Slanting orientation of methyl groups with respect to plane (020) are also consistent with the hydrophobic character of PDMS (Figure 4d).

The occurrence of specific polymer−crystal interactions at molecular level might explain the remarkable difference of

dx.doi.org/10.1021/cg4015543 | *Cryst. Growth Des.* 2014, 14, 678−686

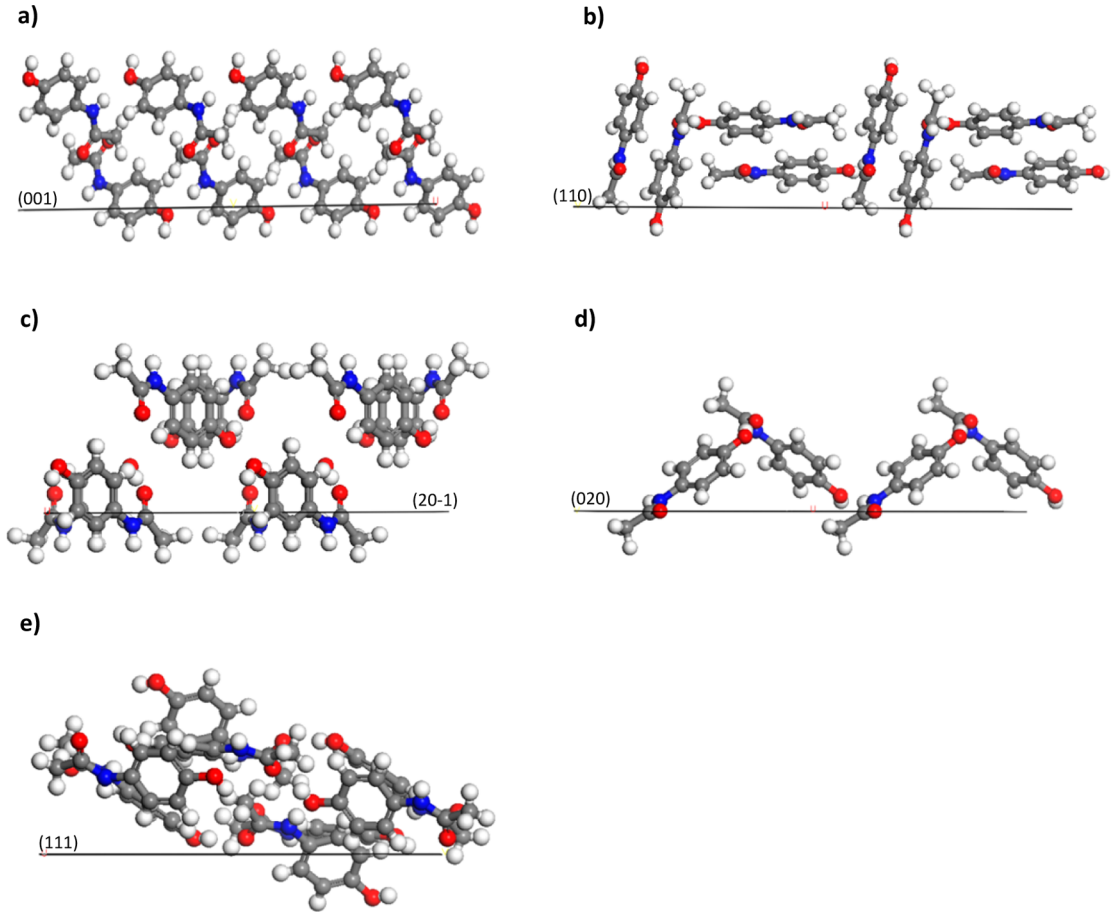

Figure 4. View of the molecular arrangement in the crystal structure of (a) monoclinic ACM along (001) face, (b) monoclinic ACM along the (110) face, (c) monoclinic ACM along the $(20\bar{1})$ face, (d) monoclinic ACM along the (020) face, and (e) orthorhombic ACM along the (111) face. ○: Hydrogen, ●: oxygen, ●: nitrogen,●: carbon. Ball-and-stick model: hydrogen (white), oxygen (red), nitrogen (blue), carbon (gray).

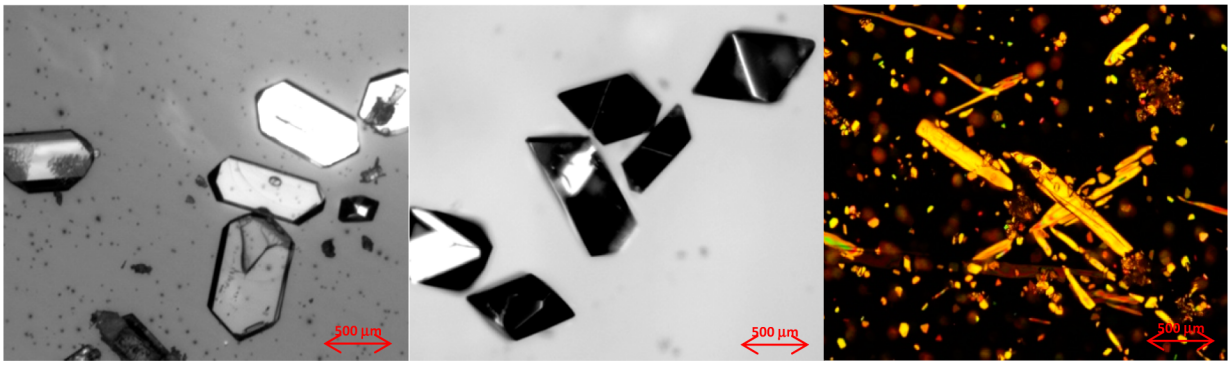

Figure 5. Left: ACM crystals with preferred orientation along the (001) face grown on the EAA surface. Center: ACM crystals on the PDMS surface. Right: concomitant crystallization of monoclinic form I (stable) and orthorhombic form II (metastable) of ACM on the PI surface.

ACM nucleation kinetics on EAA surface with respect to PDMS surface.

The PXRD pattern of ACM crystals grown on PS does not give evidence of PO.

The PXRD diffractogram of P*n*BMA shows a similar behavior, and the presence of significant peaks at 12.1° (110) and 24.4° (220) confirms that mixed hydrophobic−hydrophilic interactions occur along the direction {110} (Figure 4b). The absence of specific hydrogen-bonding interactions is consistent with the observation that the PnBMA surface is dominated by terminal methyl groups of the ester side chain when in contact with water.[31] In this case, the different nucleation kinetics between PS and P*n*BMA might be attributed to the dissimilar acid−base contributions to surface energy, as discussed in the previous section. Crystals nucleated on PVDF surfaces show a surprising orientation along the direction {001} as proved by the predominant peak in the PXRD pattern at 13.9° (001) in 2θ. This result has been confirmed by five independent experiments. The strong directional orientation might be attributed to the formation of hydrogen-bonds between the electronegative fluorine in the PVDF polymer and the hydrogen in the hydroxyl group of the ACM molecule (Figure

dx.doi.org/10.1021/cg4015543 | *Cryst. Growth Des.* 2014, 14, 678−686

4a). However, the possibility that covalently bounded fluorine acts as hydrogen-bond acceptor is still debated among experts with contrasting results. Dunitz and Taylor (1997) showed that statistical analysis of structural data and detailed inspection of individual crystal structures collected in the Cambridge Structural Database and in the Brookhaven Protein Data Bank, in conjunction with molecular orbital calculations on model systems using the *ab initio* intermolecular perturbation theory, reveal that covalently bound fluorine hardly ever acts as a hydrogen-bond acceptor.[32] On the other hand, the non-covalent interactions involving organic fluorine in partially fluorinated compounds, and their importance and versatility in supramolecular chemistry, have been recently discussed by Chopra (2012), leading to the conclusion that organic fluorine might be polarizable.[33]

PXRD patterns of ACM crystals nucleated on the PI surface revealed the concomitant presence of both the metastable polymorph II (orthorhombic) and the stable form I (monoclinic). In agreement with the hydrophilic character of PI, the major reflection at 13.9° corresponds to the preferential orientation of form I crystals along {001} with hydroxyl groups of ACM oriented toward the polymeric surface (Figure 4a). The major reflection at 15.0° is related to the preferential growth of form II crystals along the plane (111) with hydroxyl groups of ACM obliquely oriented toward the substrate (Figure 4e). Interfacial interactions are likely to involve both imide functionality and carbonyl groups in polyimide. ACM form II was observed as the first crystallizing polymorph, rearranging in time into the most thermodynamically stable form I (Figure 5).

CONCLUSIONS

This work highlights the critical role of surface chemistry in controlling the heterogeneous nucleation kinetics of ACM crystals. The experimental investigation provides evidence for the ability of some investigated amorphous polymeric films to promote specific intermolecular interactions, to generate hydrogen-bonding networks, and to induce preferred spatial orientations of solute molecules in the proximity of solid surfaces; all these aspects seem to have a significant impact on the nucleation rate and, consequently, on the whole crystallization process. This regulation approach is of particular interest due to the large variability and rather simple tunability of physicochemical and morphological properties of polymer surfaces.

Crystallization tests carried out on six polymeric substrates proved that nucleation is significantly retarded on surfaces that are not able to promote specific directional interactions between polymeric substrate and aggregating ACM molecules. On the contrary, an enhanced nucleation activity is observed concomitantly with a high value of γ_s^- (Lewis base character of the solid polymer) and with the evidence of preferred orientations of ACM crystals facets.

Under the assumption that molecules require reorganization and alignment prior to forming a critical nucleus having the same internal orientation as the bulk crystal,[34] solid surfaces able to promote an ordered rearrangement of molecules at polymer−solution interface lead to a faster nucleation process.

AUTHOR INFORMATION

Corresponding Author

*Tel.: 617-452-3790; e-mail: myerson@mit.edu.

Notes

The authors declare no competing financial interest.

ACKNOWLEDGMENTS

The financial support of Massachusetts Institute of Technology-MISTI Global Seed Fund 2012-2013 "Inhibition of Nucleation Through Surface Modification" is gratefully acknowledged.

REFERENCES

(1) Myerson, A. S. In *Handbook of Industrial Crystallization*; Butterworth-Heinemann: Waltham, MA, 2002.
(2) Tzotzi, C.; Pahiadaki, T.; Yiantsios, S. G.; Karabelas, A. J.; Andritsos, N. *J. Membr. Sci.* **2007**, *296*, 171−184.
(3) Andritsos, N.; Karabelas, A. J. *Int. J. Heat Mass Transfer* **2003**, *46*, 4613−4627.
(4) Kawasaki, K.; Buchanan, A. V.; Weiss, K. M. *Annu. Rev. Genet.* **2009**, *43*, 119−142.
(5) Grzesiak, A. L.; Uribe, F. J.; Ockwig, N. W.; Yaghi, O. M.; Matzger, A. J. *Angew. Chem., Int. Ed.* **2006**, *45*, 2553−2556.
(6) Fermani, S.; Falini, G.; Minnucci, M.; Ripamonti, A. *J. Cryst. Growth* **2001**, *224*, 327−334.
(7) Miyaji, F.; Iwai, M.; Kokubo, T.; Nakamura, T. *J. Mater. Sci. - Mater. Med.* **1998**, *9*, 61−65.
(8) Diao, Y.; Myerson, A. S.; Hatton, T. A.; Trout, B. L. *Langmuir* **2011**, *27*, 5324−5334.
(9) (a) López-Mejías, V.; Knight, J. L.; Brooks, C. L.; Matzger, A. J. *Langmuir* **2011**, *27*, 7575−7579. (b) McClelland, A. A.; López-Mejías, V.; Matzger, A. J.; Chen, Z. *Langmuir* **2011**, *27*, 2162−2165.
(10) López-Mejías, V.; Kampf, J. W.; Matzger, A. J. *J. Am. Chem. Soc.* **2012**, *134*, 9872−9875.
(11) Curcio, E.; Fontananova, E.; Di Profio, G.; Drioli, E. *J. Phys. Chem. B* **2006**, *110*, 12438−12445.
(12) Curcio, E.; Curcio, V.; Di Profio, G.; Fontananova, E.; Drioli, E. *J. Phys. Chem. B* **2010**, *114/43*, 13650−13655.
(13) Di Profio, G.; Fontananova, E.; Curcio, E.; Drioli, E. *Cryst. Growth Des.* **2012**, *12*, 3749−3757.
(14) Chunsrivirot, S.; Diao, Y.; Trout, B. L. *Langmuir* **2011**, *27*, 12381−12395.
(15) Chunsrivirot, S.; Santiso, E.; Trout, B. L. *Langmuir* **2011**, *27*, 12396−12404.
(16) van Oss, C. J.; Chaudhury, M. K.; Good, R. J. *Adv. Colloid Interface Sci.* **1987**, *28*, 35−64.
(17) Granberg, R. A.; Rasmuson, A. C. *J. Chem. Eng. Data* **1999**, *44*, 1391−1395.
(18) Kwok, D. I.; Neumann, A. W. *Can. J. Chem. Eng.* **1996**, *74*, 551−553.
(19) Jiang, S.; ter Horst, J. H. *Cryst. Growth Des.* **2011**, *11*, 256−261.
(20) Trasi, N. S.; Taylor, L. S. *CrystEngComm* **2012**, *14*, 5188−5197.
(21) Rieke, P. C. *J. Cryst. Growth* **1997**, *182*, 472−484.
(22) Alhalaweh, A.; Vilinska, A.; Gavini, E.; Rassu, G.; Velaga, S. P. *AAPS PharmSciTech* **2011**, *12*, 1186−1192.
(23) De Bartolo, L.; Morelli, S.; Rende, M.; Gordano, A.; Drioli, E. *Biomaterials* **2004**, *25*, 3621−3629.
(24) Martinelli, E.; Suffredini, M.; Galli, G.; Glisenti, A.; Pettitt, M. E.; Callow, M. E.; Callow, J. A.; Williams, D.; Lyall, G. *Biofouling* **2011**, *27/5*, 529−541.
(25) Wu, S. In *Polymer Interface and Adhesion*; Marcel Dekker: New York, 1982.
(26) Pritykin, L. M. *J. Colloid Interface Sci.* **1986**, *112*, 539−543.
(27) Morra, M.; Della Volpe, C.; Siboni, S. In *Polymer Interfaces and Emulsions*; Marcel Dekker: New York, 1999.
(28) Gotoh, K. In *Polymer Surface Modification: Relevance to Adhesion*; VSP: Utrecht, 2004.
(29) Lloyd, T. B.; Coleman, J. A. In *Acid-Base Interactions*; VSP: Zeist, 2000.
(30) Diao, Y.; Helgeson, M. E.; Siam, Z. A.; Doyle, P. S.; Myerson, A. S.; Hatton, T. A.; Trout, B. L. *Cryst. Growth Des.* **2012**, *12*, 508−517.

(31) Chen, Z.; Shen, Y. R.; Somorjai, G. A. *Annu. Rev. Phys. Chem.* **2002**, *53*, 437−465.
(32) Dunitz, J. D.; Taylor, R. *Chem.—Eur. J.* **1997**, *3*, 89−98.
(33) Chopra, D. *Cryst. Growth Des.* **2012**, *12*, 541−546.
(34) Erdemir, D.; Lee, A. Y.; Myerson, A. S. *Acc. Chem. Res.* **2009**, *42/5*, 621−629.